High-Resolution Electron-Microscopy Study of Irradiation-Induced Defects in the β''' Phase of Potassium Ferrite

By Yoshio Matsui, Yoshio Bando and Yoshizo Kitami

National Institute for Research in Inorganic Materials, 1-1 Namiki, Sakura-mura, Niihari-gun, Ibaraki 305, Japan

and Robert S. Roth

Inorganic Materials Division, National Bureau of Standards, Washington, DC 20234, USA

Abstract

A high-resolution 1 MV electron-microscopy study of the β'''-type phase of potassium ferrite, with ideal formula $K_2O.4FeO.15Fe_2O_3$, is reported. The compound is beam-sensitive and readily suffers from structural degradations during TEM observations, while the isostructural aluminate (β''-alumina) is much more stable under similar irradiation conditions. The mechanisms of structural changes are discussed based on 1 MV high-resolution structure images of electron-induced defect blocks.

Introduction

In previous papers (Matsui & Horiuchi, 1977; De Jonghe, 1977; Bovin, 1978, 1979; Matsui, Horiuchi & Ohta, 1980; Otsuka & Sato, 1983), it was reported that β''-alumina (ideally: $Na_2O.MgO.5Al_2O_3$) and β''''-alumina (ideally: $Na_2O.3MgO.7Al_2O_3$), both having rhombohedral-type crystal structures (Yamaguchi & Suzuki, 1968; Bettman & Peters, 1969; Weber & Venero, 1970), are very sensitive to an intense electron beam and readily suffer from structural changes during transmission electron microscope (TEM) observations. We proposed models of the structures of the irradiation-induced defect blocks based on high-resolution 1 MV electron-microscope structure images (Matsui & Horiuchi, 1981; Matsui, 1981a). At the same time, we also found that both β-alumina (ideally: $Na_2O.11Al_2O_3$) and β'''-alumina (ideally: $Na_2O.4MgO.15Al_2O_3$), having hexagonal-type crystal structures (Beevers & Ross, 1937; Bettman & Turner, 1971), are very stable even under intense electron irradiations. We discussed the differences of the stabilities between the rhombohedral and the hexagonal types of sodium aluminates, based on the characteristic features of their original crystal structures (Matsui, 1981b).

Compounds with β-alumina-related crystal structures are also found in some ferrites and gallates (Kummer, 1972). For example, in the $K_2O–Fe_2O_3$ system (Romanov, Candela, Roth & Swartzendruber,

1979) there are two compounds, one having the β-alumina structure (ideally: $K_2O.11Fe_2O_3$) and the other the β'''-alumina structure (ideally: $K_2O.4FeO.15Fe_2O_3$). The chemical composition of the latter compound is sometimes expressed approximately as $K_2O.17Fe_2O_3$. As was the case in β-alumina-related materials, the real chemical compositions of these two compounds are reported to deviate from the ideal ones; *i.e.* the real compositions are around $K_2O.9Fe_2O_3$ and $K_2O.11Fe_2O_3$ for the β and β''' phases of potassium ferrite, respectively. The idealized crystal structure of the β'''-type of potassium ferrite, $K_2O.4FeO.15Fe_2O_3$ ($P6_3/mmc$, $a = 5\cdot9$, $c = 33$ Å), projected onto the (110) plane is given in Fig. 1, which is drawn with reference to the β'''-alumina structure given by Bettman & Turner (1971). Like the
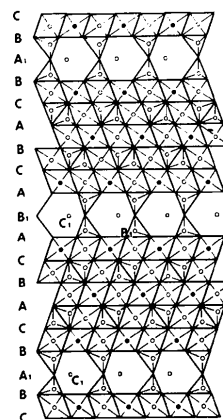

Fig. 1. The ideal crystal structure of the β''' phase of potassium ferrite, $K_2O.4FeO.15Fe_2O_3$, projected normal to the (110) plane of the hexagonal lattice ($P6_3/mmc$: $a = 5\cdot9$, $c = 33$ Å). Small squares represent K atoms in the conduction planes. Open and solid small circles indicate Fe atoms. The latter positions are occupied twice as densely as the former positions along the directions of the projections. Neighbouring spinel-like blocks are mutually related by mirror symmetry with mirror planes at the conduction planes. The symbols A_1, B_1 and C_1 indicate the positions $(0, 0, z)$, $(\frac{2}{3}, \frac{1}{3}, z)$ $(\frac{1}{3}, \frac{2}{3}, z)$, respectively. The other symbols, A_i, B_i and C_i ($i = 2$ to 4), are the positions displaced by $(\frac{1}{2}, 0, 0)$ ($i = 2$), $(0, \frac{1}{2}, 0)$ ($i = 3$) and $(\frac{1}{2}, \frac{1}{2}, 0)$ ($i = 4$) from A_1, B_1 and C_1, respectively. The symbol A, without subscripts, means that all the positions A_1 to A_4 are fully occupied.

β-alumina-related compounds, the structure of this ferrite consists of (1) spinel-like blocks and (2) so-called conduction planes. Each spinel-like block consists of six cubic-close-packed O layers. Two neighbouring spinel-like blocks are mutually related by mirror symmetry with the mirror plane at the conduction plane. The conduction planes are rather loosely packed as compared to the spinel-like blocks.

In the present study, we investigated the irradiation effects in β'''-type potassium ferrite by 1 MV high-resolution TEM (HRTEM), to compare the results with those of the aluminates previously reported. The β''' phase of potassium ferrite is very sensitive to the electron beam and suffers from structural changes during TEM observations, while the isostructural β'''-alumina itself is much more stable under similar irradiation conditions. The mechanism of the structural changes is discussed in this paper based on the high-resolution 1 MV structure images of the resultant irradiation-induced defect blocks.

Experiments and results

(1) Outline of the electron-induced damage

The β'''-type potassium ferrite examined in this study was prepared after Romanov, Candela, Roth & Swartzendruber (1979). The mixed powders (molar ratio 1:9) of K_2O and Fe_2O_3 were prepared from prereacted $KFeO_2$ and pure Fe_2O_3. The specimens were dried and sealed in a platinum tube and then heated at 1273 K for 7 h. The sample was then removed, ground and reloaded into another platinum tube. After being dried at 513 K, the tube was sealed and heated at 1748 K for 20 h followed by rapid quenching in H_2O. For TEM observations, the sample was gently crushed in CCl_4 and then dispersed on the holey-carbon film. TEM observations were made with a 1 MV high-resolution electron microscope (Hitachi: HEEM-1250) (Horiuchi, Matsui, Bando, Katsuta & Matsui, 1978).
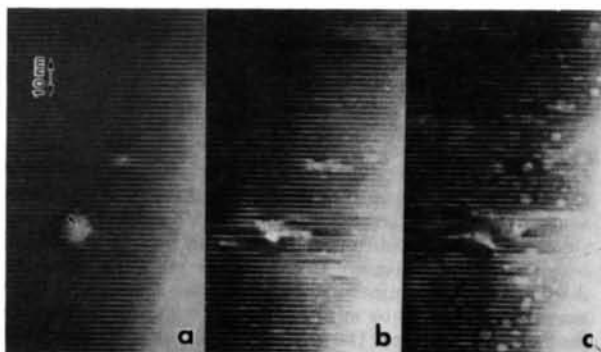
Figs. 2(a) to 2(c) show the time sequences of the structural changes in the β''' phase of potassium ferrite. The incident electron beam is normal to the (100) plane. The rows of white dots are considered to correspond to the loosely packed conduction planes which consist of K and O atoms. It is concluded from the images in (b) that some of these conduction planes are gradually eliminated and defect blocks are created as the result of the direct contact of the spinel-like blocks on either side of the lost conduction plane. Wider blocks are formed by prolonged irradiation under an intense electron beam as can be seen in the micrograph (c). It is also observed that the hole, indicated by an arrow in (a), which was accidentally included in the observed region, is gradually filled owing to atom diffusions during the electron irradiations. The hole is almost filled in the micrograph (c). The image shown in Fig. 3, on the other hand, is the result of very intense electron irradiation where the second consenser aperture of the transmission electron microscope is removed. Here almost all the conduction planes are lost and some lamellar structures are formed. The changes of the electron diffraction patterns are also shown in Figs. 4(a) to 4(c), corresponding to the images in Figs. 2(a) and 2(c) and Fig. 3, respectively. Fig. 4(a) is the $h0l$ diffraction pattern of the original β'''-ferrite. The streaks along the c^* direction observed in Fig. 4(b) are caused by the formation of irradiation-induced defects. The pattern in Fig. 4(c), which corresponds to the image in Fig. 3, exhibits a very different profile and is interpreted to be a twinned cubic crystal projected along
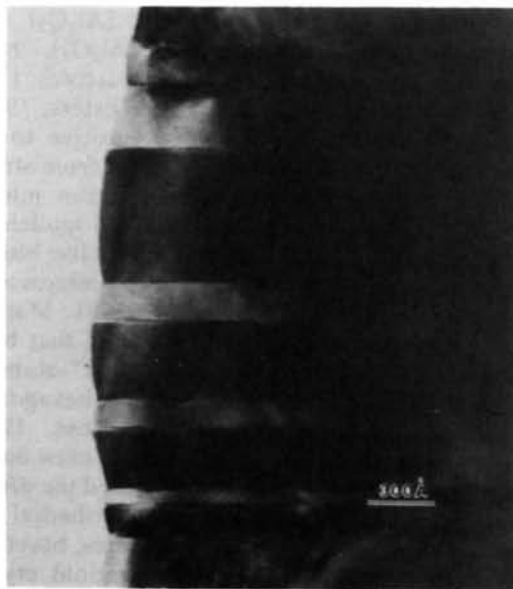

Fig. 2. 1 MV electron micrographs showing the time sequence of the development of the irradiation-induced defects in the β''' type of potassium ferrite. The incident electron beam is normal to the (100) plane.

Fig. 3. The formation of the lamellar structure as a result of the very intense electron-beam irradiation of the β''' type of potassium ferrite in 1 MV TEM. According to the electron diffraction pattern shown in Fig. 4(c), these lamellae are considered to be the twinned lamellae of magnetite (Fe_3O_4).

the common [110] direction. The lattice parameter of this cubic lattice is measured to be $a = 8.4$ Å and is reasonably assigned to magnetite (Fe_3O_4) with the spinel structure [space group $Fd3m$ with $a = 8.396$ Å (ASTM, 19-629)]. From these observations, it is clear that the β'''-type crystal of potassium ferrite gradually suffers from the loss of the conduction planes during TEM observations and finally is changed into the twin lamellae of Fe_3O_4.

(2) HRTEM investigations of the early stage of damage

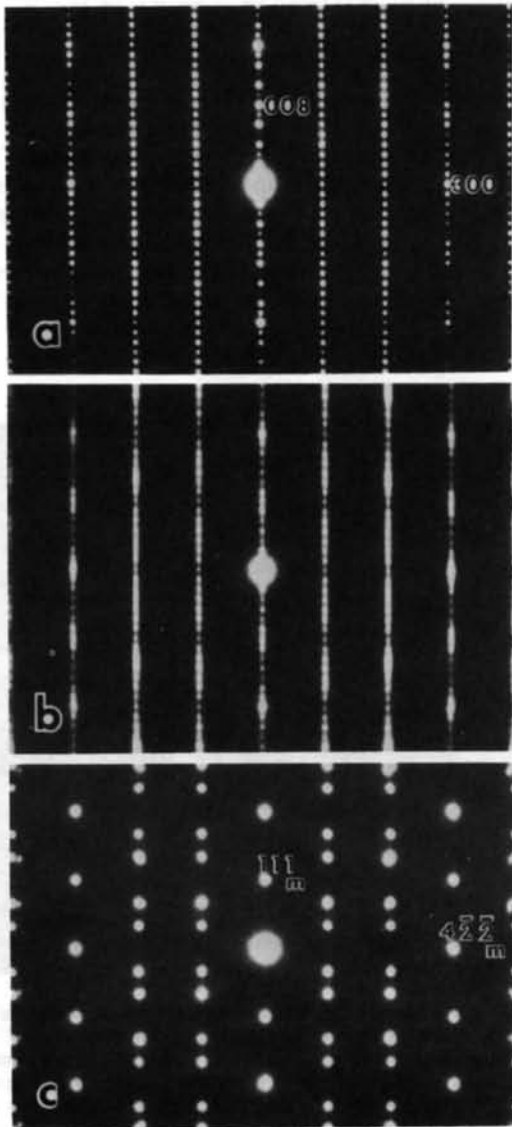Fig. 5 is the 1 MV image of the defect blocks formed by the contact of two spinel-like blocks. The image was taken with the incident beam onto the (110) plane of the host hexagonal lattice of β'''-ferrite. Originally, these two spinel-like blocks had the mutually opposite O-layer sequences ... ABCA... and ... ACBA..., respectively. From inspection of Fig. 5, these opposite sequences are considered to be kept even after they are directly combined to form defect blocks. Another image of such a defect block with the beam normal to the (100) plane is given in Fig. 6. In both Figs. 5 and 6, the upper and the lower rows of white dots corresponding to the conduction planes on both sides of the defect blocks are observed at the same x, y positions. These observations suggest that the shift vector, by which the relative displacement of the upper part of the lost conduction plane with respect to the remaining lower one is described, is just along the c axis of the original hexagonal lattice and is written as,

$$\mathbf{V}_c = -(1/14)\mathbf{c},$$

where $\mathbf{c}$ is the lattice vector of β'''-ferrite. The absolute value of $\mathbf{V}_c$ is about 2.3 Å. Resultant O-layer sequences in the defect blocks are,

$$... A_1[(CBACBA)(ABCABC)]A_1. ...$$

Here the formation of non-close-packed O layers, ... BAAB..., is assumed in the central part of the defect block.

Fig. 7 includes the defect block created by the combinations of three spinel-like blocks. In this region, zigzag sequences of the white dots, expected if the original packing sequences of O layers are
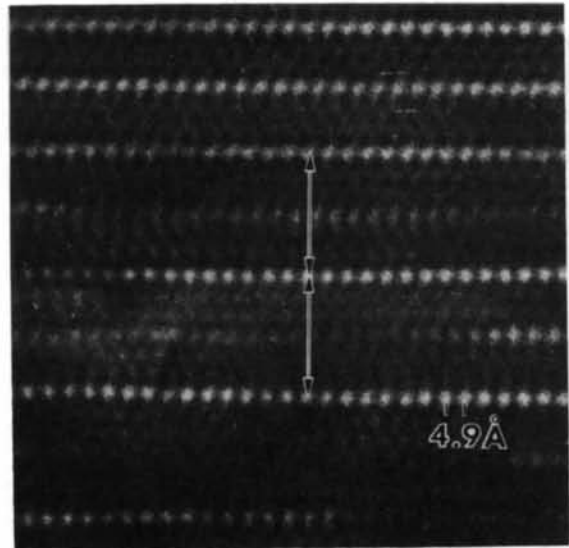

Fig. 4. Changes of the *hkl* electron diffraction pattern of the β''' type of potassium ferrite, due to the electron-beam irradiation in TEM. Patterns (*a*) to (*c*) corresponds to the images shown in Figs. 2(*a*), 2(*c*) and 3, respectively.

Fig. 5. 1 MV high-resolution TEM image of the β''' type of potassium ferrite projected onto the (110) plane. Two defect blocks are formed accidentally side by side. Each defect block is considered to be created by the direct contact of two original spinel-like blocks in the β''' structure. The original mirror symmetry is seen to be preserved even in the irradiation-induced defect blocks.

preserved, are not observed. This suggests that some rearrangements of O-layer sequences occur at this stage and small blocks with cubic close packing of 18 O layers are created. Such a block may be the small seed of the magnetite, later grown large as we have seen in Fig. 3.

Discussion

(1) Possible models of structural changes

Rearrangements of O layers

According to our experiments, it is considered that the original O-packing sequences are preserved when two spinel-like blocks are combined, while some re-arrangements of O packing occur when three blocks are combined, so that the cubic close packing of 18 O layers is realized. At the present stage, we cannot tell the detailed process of such rearrangements. Fig. 8, however, shows one of the possible atom rearrangements after the contact of three spinel-like blocks. In this figure, the directions of the displacements of both Fe and O atoms are indicated. If the original O-layer sequences in the β'''-type structure are preserved at the first step, the resultant O-layer sequence in the defect block may be

$$\ldots A_1[(CBACBA)(ABCABC)(CBACBA)]C_1.\ldots$$

It may be reasonable to expect that the underlying O layers are displaced to prevent the repetition of the same x, y positions. At the same time, two layers in the central part may also be displaced with respect
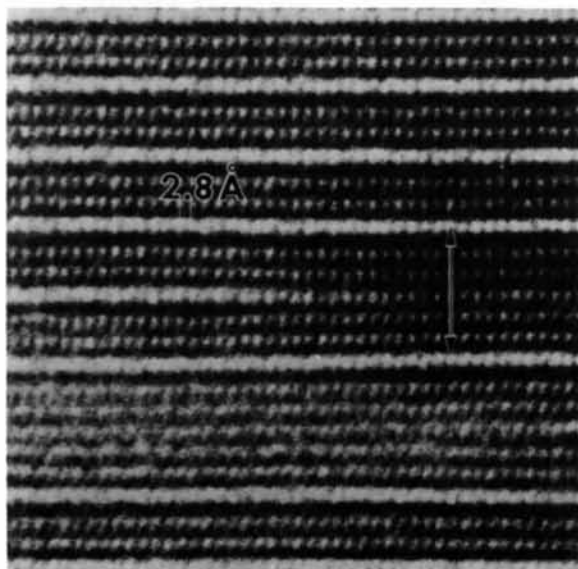
to each other and, finally, O sequences such as

$$\ldots A_1[(CBACBA)(CBACBA)(CBACBA)]C_1.\ldots$$

are created as shown in Fig. 8. In this way, small lamellae with the ... $ACBA$... type of cubic close packing of 18 O layers are created and this can be the small seed of the magnetite structure.

There is also another chance of forming the lamellae with a reversed O sequence, such as:

$$\ldots C_1[(ABCABC)(ABCABC)(ABCABC)]A_1.\ldots$$

The probabilities of forming ... $ACBA$... and ... $ABCA$... packings are the same and this may lead to the final formation of the twin lamellae of magnetite as we have seen in Fig. 3. A schematic model of such a process of twin formation is drawn in Fig. 9.

Rearrangements of Fe atoms

To obtain the spinel structure, a rearrangement of the Fe ions must also be considered, besides the changes of O-layer packing mentioned above. The possible ways for such displacements of Fe atoms to form the spinel type of structure are also indicated in Fig. 8. The magnitudes of the displacements are about 1·6 Å in this model. There remains, however, a problem with regard to the cations just next to the
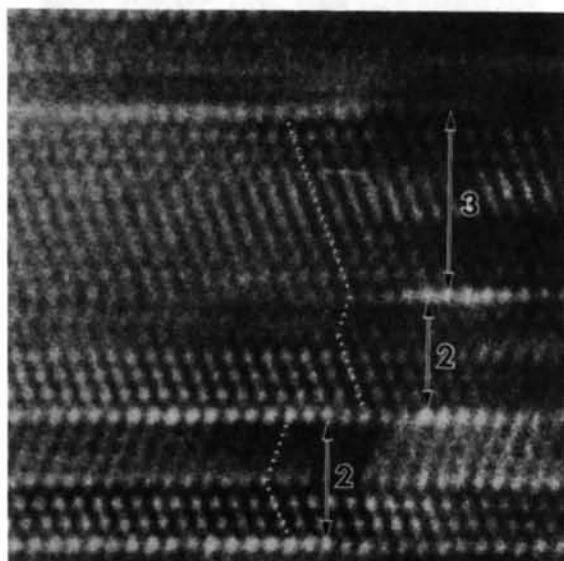

Fig. 6. 1 MV high-resolution TEM image of the β''' type of potassium ferrite projected onto the (100) plane. The upper and lower spinel-like blocks are considered to be combined directly along the c axis, without any displacements normal to the c axis, after the loss of the conduction plane between them.

Fig. 7. 1 MV image of the slightly advanced stage of damage in the β''' type of potassium ferrite projected normal to the (110) plane. In the upper region of this figure, the defect block formed by three original spinel blocks is observed. The zigzag sequence of white dots, expected from the original structure, is not observed in this region. This strongly suggests that some rearrangement of atoms takes place when three spinel-like blocks are combined, while the original structure is almost preserved at the stage of two block contacts, as can be seen in the lower part of the figure.

conduction planes, forming an Fe–O–Fe column in the original β'''-ferrite structure. In this region, the number of Fe atoms per unit cell is two, while this number is three inside the spinel-like layers. Therefore, if we consider only the intralayer cation displacements, the number of Fe atoms in those layers which were originally the conduction planes must be deficient by $\frac{1}{3}$ as compared to the remaining layers. Such Fe-deficient layers may occur once in every six layers and this would mean that a superstructure with a period of 14 Å $(6 \times 2\cdot3$ Å) must be expected. Such a superstructure is, however, not detected in either the diffraction pattern in Fig. 4(c) or in the image in Fig. 3, both of which exhibit the typical features of the twinned lamellae of Fe_3O_4. This indicates that interlayer diffusions of Fe atoms may also take place in the process of structural changes to average out the number of Fe atoms in all the cation layers in a resultant magnetite structure.

(2) Reductions of Fe^{3+} ions by the electron beam

If we assume the idealized composition $K_2O.4FeO.15Fe_2O_3$, then the ideal ratio $Fe^{2+}/Fe(total)$ is about $0\cdot118$. Because each conduction plane has the ideal composition $[KO]^-$, it is considered very difficult to eliminate the atoms in the conduction planes, maintaining the condition of charge neutrality. The reductions of some Fe^{3+} ions to Fe^{2+} ions may, therefore, occur during electron irradiation, to compensate the excess negative charge after the loss of the conduction plane with the local composition K^+O^{2-}. If the planes are lost as
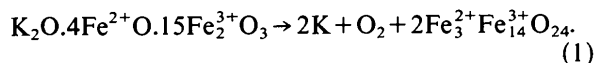
$$KO^- \rightarrow K + \tfrac{1}{2}O_2 + e^-$$
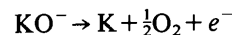
then, the excess negative charge can be compensated as

$$Fe^{3+} + e^- \rightarrow Fe^{2+}.$$
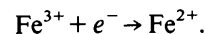
The reaction involving loss of conduction planes from ideal β'''-ferrite can then be expressed as

$$K_2O.4Fe^{2+}O.15Fe_2^{3+}O_3 \rightarrow 2K + O_2 + 2Fe_3^{2+}Fe_{14}^{3+}O_{24}.$$
$$(1)$$

The product thus obtained has the composition $Fe_{17}O_{24}$ or $Fe_{2\cdot833}O_4$, where $Fe^{2+}/Fe(total)$ is $0\cdot177$. The composition slightly deviates from the ideal one of Fe_3O_4. It is well known, however, that γ-Fe_2O_3 (maghemite) also has the spinel-like structure with cubic subcell $a = 8\cdot34$ Å (ASTM: 25-1402) and, therefore, the compound with the composition between $Fe_{2\cdot67}O_4$ and Fe_3O_4 has the possibility of crystallizing into the spinel type of structure. In this respect, the reaction (1), by which defective magnetite, $Fe_{17}O_{24}$ (or $Fe_{2\cdot833}O_4$), is obtained can explain the observed image in Fig. 3 and the electron diffraction pattern in Fig. 4(c). If, on the other hand, the final product is the stoichiometric magnetite (Fe_3O_4), further reduction must be taken into account as

$$Fe_3^{2+}Fe_{14}^{3+}O_{24} \rightarrow 0\cdot65O_2 + Fe_{5\cdot7}^{2+}Fe_{11\cdot4}^{3+}O_{22\cdot7}$$

$$(=5\cdot7Fe_3O_4).$$
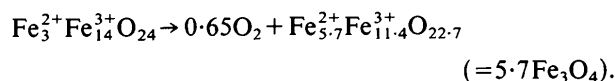
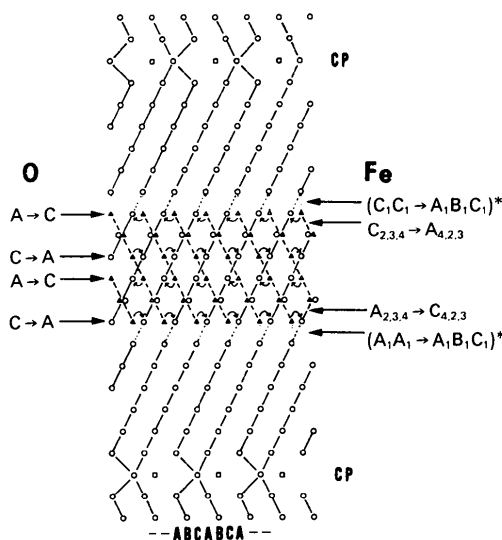The whole reaction from the β''' phase of potassium

Fig. 8. The possible models of the atom displacements to form the spinel-type structure after the contacts of three successive spinel-like blocks. Slight displacements of some O and cation layers in the central part of the defects can lead to the spinel-type structure. At the cation layer indicated by stars, the number of Fe atoms is deficient and, therefore, the interlayer diffusion of Fe atoms may occur to form finally the magnetite structure.
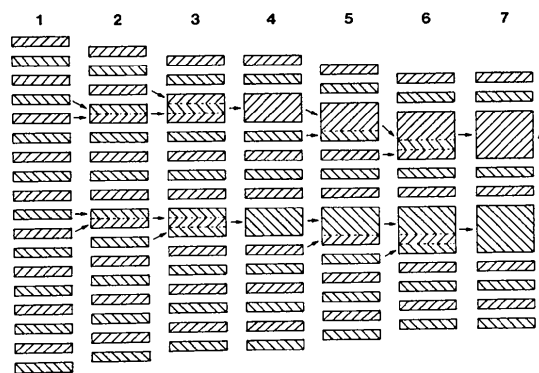

Fig. 9. The hypothetical model of the process of formation of magnetite-like layers in the β''' type of ferrite. The hatched rectangular blocks at step (1) represent the spinel-like blocks of six O layers. At step (2), some of the two neighbouring blocks are combined preserving their original packing sequences. At step (3), one more block is combined to form the zigzag O sequence. The rearrangement of atoms in the central part, however, takes place to realize the cubic close packing of 18 O layers, as shown at step (4). (Fig. 8 described the atom arrangements at this stage of structural change.) Through similar processes shown at steps (5) and (6), the small areas of spinel structures, A and B, shown at step (7), are created. Such a process may finally bring about the twinned lamellae of magnetite as already shown in Fig. 3.

ferrite to stoichiometric magnetite would be

$$K_2O.4FeO.15Fe_2O_3 \rightarrow 2K + 2 \cdot 3O_2 + 11 \cdot 3Fe_3O_4. \quad (2)$$
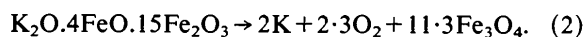
Both equations (1) and (2) are based on the ideal compositions of β'''-ferrite. Slight changes of the coefficients will of course be required when we consider the real compositions of the material.

At the present stage, it is very difficult to discuss how the potassium atoms are lost from the crystal in the electron beam. Perhaps K^+ ions are reduced to metallic potassium, as indicated in both equations (1) and (2), and then lost by sublimation into the vacuum of the electron microscope. The rise of temperature caused by the electron beam may partly assist such sublimation. In the case of Ag β-alumina, formation of Ag whiskers upon electron irradiation was observed (Roth, 1972).

(3) Comparisons with β'''-alumina

TEM observations of damage in β-alumina-type compounds were reported by Otsuka & Sato (1983). In general, however, β- and β'''-alumina with hexagonal structures are known to be very stable under the ordinary electron-illumination condition of HRTEM, as compared to rhombohedral counterparts (De Jonghe, 1977; Matsui, 1981b). TEM observations of β''-alumina are also reported by Hull, Smith & Humphreys (1983). They found some defects in β'''-alumina but they are considered to be intrinsic defects and not the results of electron damge (D. J. Smith, private communication).

These differences of the structural stabilities between β''' types of aluminates and ferrites may be explained as follows. As mentioned before (Matsui, 1981b), the high sensitivity of rhombohedral β''- and β''''-aluminas can be attributed to the fact that each conduction plane has the ideal local composition $[Na_2O]^0$ (real composition about $[Na_{1\cdot67}O]^{0\cdot33-}$) and, therefore, the charge neutrality can be maintained easily even when the atoms in the conduction planes are released out of the structures. In the case of hexagonal β- and β'''-aluminas, on the other hand, the corresponding ideal local composition is $[NaO]^{1-}$ (real composition about $[Na_{1\cdot33}O]^{0\cdot67-}$) and, therefore, it is not as easy to keep the charge balance when the atoms in the conduction planes are lost by electron irradiation. This means that it is more difficult to release the atoms in the conduction planes out of the

structures and this may be the reason that the hexagonal β- and β'''-alumina hardly suffer from degradation even under intense electron irradiation. The situation is, however, changed in ferrites with β or β''' types of structures, because charge neutrality after the release of atoms in the conduction planes can be maintained by the additional reduction of some Fe^{3+} to Fe^{2+} ions as mentioned above. Occurrences of such reductions are hardly expected for Al^{3+} ions in aluminates. This may be the principal reason why the β''' phase of ferrite is very sensitive to the electron beam and readily suffers from structural changes, while the isostructural β''' phase of the aluminate is quite stable under similar irradiation conditions. It may be worth noting that such a reduction of Fe^{3+} ions by the electron beam is also discussed in the case of Fe-stabilized β''-alumina (Otsuka & Sato, 1983).

References

BEEVERS, C. A. & ROSS, M. A. (1937). Z. Kristallogr. 97, 59–66.
BETTMAN, M. & PETERS, C. R. (1969). J. Phys. Chem. 73, 1774–1780.
BETTMAN, M. & TURNER, L. L. (1971). Inorg. Chem. 10, 1442–1446.
BOVIN, J.O. (1978). Nature (London), 273, 136–138.
BOVIN, J.-O. (1979). Acta Cryst. A35, 572–580.
DE JONGHE, L. C. (1977). Mater. Res. Bull. 12, 667–674.
HORIUCHI, S., MATSUI, Y., BANDO, Y., KATSUTA, T. & MATSUI, I. (1978). J. Electron Microsc. 27, 39–48.
HULL, R., SMITH, D. J. & HUMPHREYS, C. J. (1983). J. Microsc. 130, 203–214.
KUMMER, J. T. (1972). Prog. Solid State Chem. 7, 141–175.
MATSUI, Y. (1981a). J. Appl. Cryst. 14, 38–42.
MATSUI, Y. (1981b). Solid State Ionics, 3/4, 135–140.
MATSUI, Y. & HORIUCHI, S. (1977). Proceedings of the 5th International Conference on High Voltage Electron Microscopy, Kyoto, pp. 321–324. Tokyo: Japanese Society of Electron Microscopy.
MATSUI, Y. & HORIUCHI, S. (1981). Acta Cryst. A37, 51–61.
MATSUI, Y., HORIUCHI, S. & OHTA, T. (1980). J. Solid State Chem. 32, 181–184.
OTSUKA, N. & SATO, H. (1983). Solid State Ionics, 9/10, 169.
ROMANOV, V. P., CANDELA, G. A., ROTH, R. S. & SWARTZENDRUBER, L. J. (1979). J. Appl. Phys. 50, 6455–6458.
ROTH, W. L. (1972). Natl Bur. Stand. (US) Spec. Publ. 364.
WEBER, N. & VENERO, A. (1970). Paper 1-JV-70. Proc. 72nd Annu. Meet. Am. Ceram. Soc., Philadelphia.
YAMAGUCHI, G. & SUZUKI, K. (1968). Bull. Chem. Soc. Jpn, 41, 93–99.